ESA ESTEC
Keplerlaan 1
2201 AZ Noordwijk
The Netherlands

ENVISION SAR POINTING REQUIREMENTS JUSTIFICATION (PRJ)

Prepared by Envision Study Team
ESTEC

Document Type RQ
Reference ESA-ENVIS-EST-MIS-RS-010
Issue/Revision 1.1
Date of Issue 08/07/2022
Status Draft

Table of Contents

1. APPLICABLE AND REFERENCE DOCUMENTS

1.1. Applicable Documents

[AD1] *EnVision Mission Analysis Guidelines*. Tech. rep. ESA-ENVIS-ESOC-MIS-AN-001.

[AD2] *EnVision Science Operations Reference Scenario*. Tech. rep. ESA-ENVIS-EST-MIS-TN-001.

[AD3] *Mission Requirements Document*. Tech. rep. ESA-ENVIS-EST-MIS-RS-001.

[AD4] EnVisionTeam. *EnVision Acronyms Terms and Definition for Phase B1*. Tech. rep. TBW. 2022.

[AD5] *EnVision Payload Definition Document (VenSAR)*. Tech. rep. ESA-ENVIS-JPL-PL-RS-001.

[AD6] *Mission Requirements Document*. Tech. rep. ESA-ENVIS-EST-MIS-RS-001.

1.2. Reference Documents

[RD1] *EnVision Covariance Analysis on the Science Orbit*. Tech. rep. ESA-ENVIS-ESOC-GS-HO-001.

[RD2] M.A. Wieczorek. "Gravity and Topography of the Terrestrial Planets". In: Jan. 2015, pp. 153–193. DOI: 10.1016/B978-0-444-53802-4.00169-X.

[RD3] R. Keith Raney. "Doppler properties of radars in circular orbits". In: *International Journal of Remote Sensing* 7 (1986), pp. 1153–1162.

[RD4] Sung-Hoon Mok et al. "Roll Steering of Yaw–Pitch Steered SAR for Reducing Ground–Target Pointing Error". In: *IEEE Geoscience and Remote Sensing Letters* 15.1 (2018), pp. 38–42. DOI: 10.1109/LGRS.2017.2772245.

[RD5] Daniel P. Scharf. "Analytic Yaw–Pitch Steering for Side-Looking SAR With Numerical Roll Algorithm for Incidence Angle". In: *IEEE Transactions on Geoscience and Remote Sensing* 50.9 (2012), pp. 3587–3594. DOI: 10.1109/TGRS.2012.2183375.

[RD6] H. Fiedler et al. "Total zero Doppler Steering-a new method for minimizing the Doppler centroid". In: *Geoscience and Remote Sensing Letters, IEEE* 2.2 (Apr. 2005), pp. 141–145. ISSN: 1545-598X. DOI: 10.1109/LGRS.2005.844591.

[RD7] E. Boerner et al. "A new method for Total Zero Doppler Steering". In: *IGARSS 2004. 2004 IEEE International Geoscience and Remote Sensing Symposium*. Vol. 2. 2004, 1526–1529 vol.2. DOI: 10.1109/IGARSS.2004.1368712.

[RD8] Logsdon Tom. *Orbital Mechanics : Theory and Applications*. New York: J. Wiley., 1998.

[RD9] I. S. Gradshteyn and I. M. Ryzhik. *Table of Integrals, Series and Products*. sixth. New York: Academic Press, 2000.

2. INTRODUCTION

Six categories of SAR-driven pointing-related mission performance requirements (level 1) have been specified in [AD3] (MRD), derived from the Science requirements of the mission. These requirements have been flown-down in [AD3] to Level 2 requirements toward S/C, SAR instrument, Mission Operations Ground Segment (MOC), and Science Operations Planning (SOC).

The present document provides a justification of the related MRD requirements, of their flow-down from level 1 to 2 and provides a justification for the apportionment of the various Level 2 contributors.

Acronyms, notation and reference systems (VCI, VCR, SC, OE, TCN, tcn, DAEU, AAEU) are defined in [AD4].

Reference [AD4] also contains definitions and illustrations for $\mathbf{t}_i(t)$, $\mathbf{c}_i(t)$, $\mathbf{n}_i(t)$, $\mathbf{t}_o(t)$, $\mathbf{c}_o(t)$, $\mathbf{n}_o(t)$, $\mathbf{I}_2$, $\mathbf{Q}_2$, $\mathbf{M}_i(\theta_i)$, $\mathbf{M}(t)$, ω_p, ω_o, ω, θ_i, $\beta(t)$, ξ, $R(t)$, $\hat{\mathbf{a}}_i(t)$, $\hat{\mathbf{u}}_i(t)$, $\hat{\mathbf{e}}_i(t)$, $\underline{\hat{\mathbf{a}}}_i(t)$, $\underline{\hat{\mathbf{u}}}_i(t)$, $\underline{\hat{\mathbf{e}}}_i(t)$, $\hat{\mathbf{u}}_p(t)$, $\mathbf{x}_p(t)$, $\mathbf{x}_i(t)$, and $\gamma(t)$.

3. IDEAL STEERING

This section discusses three geometrical steering conditions that simplify imaging and signal processing demands for a satellite-based SAR. These conditions include zero-Doppler steering, elevation steering and azimuth steering. It should be noted that ideal azimuth steering implies zero-Doppler steering.

3.1. Zero-Doppler Steering

3.1.1. Requirement justification

Imaging in the so called zero-Doppler configuration provides signal processing simplifications and adds robustness to the image formation process and thus is preferred by many SAR systems including VenSAR. As per [AD5], in an ideal case (perfectly spherical non-rotating planet and a perfectly circular orbit) then pointing perpendicular to the inertial velocity vector, which is also the Venus body fixed velocity in this case, would give the desired zero-Doppler geometry for the VenSAR instrument. Although we can assume Venus is roughly spherical in shape the planet rotation is not zero and EnVision's orbit is not circular. The SAR antenna boresight needs therefore to be actively controlled to permanently point toward the zero-doppler direction. The antenna being rigidly attached to the S/C, this pointing control is provided by the S/C and its attitude control system.

The doppler effect $f_d(t)$ for the SAR at time t is the derivative with respect to the time of the

phase, and is given by the following equation:

$$f_d(t) = \frac{2}{\lambda}\hat{\mathbf{u}}_p^T(t)\dot{\mathbf{x}}_p(t) \tag{1}$$

where

- $\dot{\mathbf{x}}_p(t)$ is the SC velocity vector wrt a VCR frame
- λ is the SAR wavelength
- $\hat{\mathbf{u}}_p(t)$ is the unit line of sight vector or slant range vector from SAR focal point to target on the surface of Venus.

The zero-Doppler condition is therefore given by:

$$\hat{\mathbf{u}}_p^T(t)\dot{\mathbf{x}}_p(t) = 0. \tag{2}$$

Since attitude steering is commanded on the satellite in inertial space, the zero-Doppler condition has to be transformed into a condition in inertial space that, when transformed to the VCR frame, leads to the above relation. By using the relation between the VCR and VCI reference frames, the zero-Doppler condition may be written as:

$$\hat{\mathbf{u}}_i^T(t)\left[\omega_p\mathbf{Q}_2\mathbf{x}_i(t) + \dot{\mathbf{x}}_i(t)\right] = 0, \tag{3}$$

where

- $\hat{\mathbf{u}}_i(t)$ is the SAR line of sight vector expressed in the VCI frame
- $\mathbf{x}_i(t)$ and $\dot{\mathbf{x}}_i(t$ are the SC position and velocity expressed in the VCI frame
- ω_p is the rotation rate of the planet in radians/second
- and

$$\mathbf{Q}_2 = \begin{bmatrix} 0 & 1 & 0 \\ -1 & 0 & 0 \\ 0 & 0 & 0 \end{bmatrix}.$$

Because ω_p is so small for Venus, assuming that it is zero leads to a residual Ddoppler error in azimuth, estimated to be maximum $1/50^{\text{th}}$ of the azimuth beamwidth. Although this is considered small enough to be ignored ([AD5]), (3) is the most general form of the zero-Doppler condition.

This level 1 requirement is flown-down to the following requirement:

- R-SYS-ACS-0161

3.2. Elevation Steering

3.2.1. Requirement justification

To capture the desired image swath, the boresight must be steered in elevation and, depending on the imaging geometry, echo window timing must be correctly adjusted.

For a perfectly circular orbit around a perfectly spherical planet, both the boresight elevation steering and the echo window timing remain constant for the duration of the SAR pass. In such a case, the elevation steering angle and echo window timing would depend on the desired swath and associated satellite to swath range.

Although Venus is sufficiently spherical for constant elevation steering, the satellite orbits under consideration force consideration of dynamic elevation steering and, depending on the steering, also dynamic adjustment of the echo window timing during the SAR acquisition. More specifically, a dynamic elevation steering law can be constructed to allow for constant echo window timing. This dynamic steering law may be expressed as:

$$-\hat{\mathbf{u}}_p^T(t)\hat{\mathbf{x}}_p(t) = v(t), \tag{4}$$

where $\hat{\mathbf{u}}_p(t)$ and $\hat{\mathbf{x}}_p(t)$ denote unit vectors in the respective directions and $v(t)$ denotes the cosine of the varying off-nadir angle (the negative sign arises because the satellite position vector points from the center of the planet to the satellite). The function $v(t)$ may be chosen to ensure that the center of the swath is measured with a constant incidence angle, so that the range to the center of the swath does not change over azimuth, or that the depression angle is kept constant. In the inertial frame the above corresponds to

$$\hat{\mathbf{u}}_i^T(t)\hat{\mathbf{x}}_i(t) = -v(t). \tag{5}$$

3.3. Azimuth Steering

3.3.1. Requirement justification

With three degrees of freedom, equations (3) and (5), along with the unit vector condition, completely specify $\hat{\mathbf{u}}_i(t)$. One notes, however, that $\hat{\mathbf{u}}_i(t)$ remains invariant under any rotation of the satellite around $\hat{\mathbf{u}}_i(t)$.

For a circularly symmetric antenna pattern, this rotation would have no impact. The Envision SAR reflector, however, has a significantly shorter elevation than azimuth dimension, and thus the effect of the rotation cannot be ignored. Specifically, although $\hat{\mathbf{u}}_i(t)$ satisfies (3), the Doppler centroid away from boresight (in elevation) can wander from zero.

In order to avoid the effects of such a rotation, attitude steering should also require that $\hat{\mathbf{a}}_i(t)$

aligns with the VCI representation of the unit vector in the direction of $\dot{\mathbf{x}}_p(t)$.

3.4. Analytic Beam Pointing Rule

As derived in Section B, requirements for zero-Doppler, elevation and azimuth steering lead to the following solutions (with plus and minus corresponding to left or right looking)

$$\hat{\mathbf{u}}_i(t) = \begin{bmatrix} -v(t)\sin\gamma(t) + \frac{v(t)D(t)F(t)\cos\gamma(t)\sin\gamma(t)}{F^2(t)+[\sin\theta_i\cos\beta(t)]^2} \pm s_2(t)\cos\gamma(t)\cos\beta(t)\sin\theta_i \\ -\frac{v(t)D(t)\sin\theta_i\sin\gamma(t)\cos\beta(t)}{F^2(t)+[\sin\theta_i\cos\beta(t)]^2} \pm s_2(t)F(t) \\ v(t)\cos\gamma(t) + \frac{v(t)D(t)F(t)\sin^2\gamma(t)}{F^2(t)+[\sin\theta_i\cos\beta(t)]^2} \pm s_2(t)\sin\gamma(t)\cos\beta(t)\sin\theta_i \end{bmatrix} \tag{6}$$

where

- $D(t) = \frac{\omega_o(t)}{\omega_p}$,
- $\omega_o(t)$ is the instantaneous orbit radial speed (radians/second),
- θ_i is the orbit inclination angle,
- $F(t) = D(t)\cos\gamma(t) - \cos\theta_i$,
- $s_2(t) = \frac{\sqrt{(1-v^2(t))\left[\sin^2\theta_i\cos^2\beta(t)+F^2(t)\right]-v^2(t)\sin^2\gamma(t)}}{\sin^2\theta_i\cos^2\beta(t)+F^2(t)}$,
- $\cos\gamma(t) = \frac{1+e\cos[\beta(t)-\omega]}{\sqrt{1+2e\cos[\beta(t)-\omega]+e^2}}$,
- $\sin\gamma(t) = \frac{e\sin[\beta(t)-\omega]}{\sqrt{1+2e\cos[\beta(t)-\omega]+e^2}}$,
- e is the orbit eccentricity,
- $\beta(t)$ is the orbit angle (See figure 3 in [AD4]),
- ω is the argument of perigee.

Additionally, Section B shows that on should choose

$$\hat{\mathbf{a}}_i(t) = \frac{1}{|\mathbf{A}_z(t)|}\begin{bmatrix} D(t) - \cos\gamma(t)\cos\theta_i \\ -\cos\beta(t)\sin\theta_i \\ -\sin\gamma(t)\cos\theta_i \end{bmatrix}. \tag{7}$$

where

- $|\mathbf{A}_z(t)| = \sqrt{D^2(t) - 2D(t)\cos\gamma(t)\cos\theta_i + \cos^2\theta_i\sin^2\beta(t) + \cos^2\beta(t)}$.

4. ATTITUDE CONTROL

Known desired $\hat{\mathbf{u}}_i(t)$ and $\hat{\mathbf{a}}_i(t)$, from (6) and (7), respectively, allow complete definition of the DEAU frame at any time, t. The section titled, "Transformation from DAEU to desired SC frame" in [AD4] then permits computation of the required, ideal, SC basis vectors, $\hat{\mathbf{i}}_s(t)$, $\hat{\mathbf{j}}_s(t)$ and $\hat{\mathbf{k}}_s(t)$.

Attitude control aims, through roll, pitch and yaw control defined in the order detailed in [AD4], section (5.3), to orient the spacecraft to satisfy the given $\hat{\mathbf{i}}_s(t)$, $\hat{\mathbf{j}}_s(t)$ and $\hat{\mathbf{k}}_s(t)$. Note that these are not the roll, pitch and yaw angles that would be needed to rotate the spacecraft from a default "aligned with the VCI frame" into the desired. Instead, **by definition**, they are the roll, pitch and yaw angles that would be needed to transform the tcn frame into the SC frame. The precise definition of roll, pitch and yaw angles is provided in Section 5 of [AD4].

The relations defined in (76) and (82) allow computation of the DAEU reference frame through definition of the orbit paramters and either the orbit angle or the time elapsed since the satellite passed the ascending node. The guidance laws thus rely on the Keplerian orbit model and errors between this ideal model and reality will manifest as errors in zero-Doppler steering and/or errors in placement of the swath.

More specifically, the DAEU frame may be computed by using the parameters in Table 1.

Parameter	Symbol
Eccentricity	e
Angle of perigee	ω
Semi-major axis	a
Inclination angle	θ_i
Gravitation constant	G
Mass of planet	M
Planet rotation rate	ω_p
Orbit angle	$\beta(t)$

Table 1: Input parameters

With these input parameters, the quantities in (112), (113), (102) and (103) can be computed. These, in turn, can be utilized by (72) to compute $s(t)$. Finally, $s(t)$, and the computed quantities can be inserted into (76) and (82).

5. ELEVATION, AZIMUTH AND TILT ANGLE ERRORS

As reported in [AD4], the AAEU frame represents the actual beam, azimuth and elevation frame rather than the desired (DAEU).

Large differences between the AAEU and DAEU frames directly impact the capability to meet mission requirement R-MIS-PER-1045 - that the azimuth and elevation beams should be steered with an accuracy of better than 1/15 of the beamwidths in each respective direction.

This section recasts the azimuth beam requirement as an equivalent Doppler centroid requirement, and elevation beam requirement as an equivalent swath placement requirement. Specifically, Requirement R-MIS-PER-1045 has been interpreted as follows: the actual 3dB across-track footprint of the beam must intersect with the desired/ideal 3dB across-track footprint by at least 14/15 for 95% of all measurements and the absolute value of the Doppler centroid for all ranges in the across-track 3dB footprint must be less than 1/15 of the Doppler bandwidth for 95% of all measurements.

As illustrated in Figure 1, the ”all ranges” condition imposes a requirement on the allowable tilt angle error, $\tau(t)$. Extreme values of the Doppler centroid will be found at the near or far range.

5.1. Simulation to Determine Effect of Pointing Error Contributions

The azimuth, elevation and title angle errors, $\alpha(t)$, $\epsilon(t)$ and $\tau(t)$, as defined in [AD4], section 7, relate the AAEU frame to the DAEU frame. These errors are modelled as Gaussian random vector processes over t and relate to the so-called Absolute Performance Error (APE). Specifically, they are modelled as zero-mean with some covariance matrix, $\mathbf{R}_{\text{aeu}}(t)$, that reflects the various statistically independent contributions to their random nature.

Performance is simulated as follows:

1. A state vector at time, t, is randomly selected from a provided orbit file.
2. Keplerian orbit parameters are estimated from the provided state vector
3. The Keplerian orbit parameters, (Table 1), are used to compute the DEAU basis vectors
4. For given $\mathbf{R}_{\text{aeu}}(t)$
   (a) AAEU is generated with random values of $\epsilon(t)$, $\alpha(t)$ and $\tau(t)$ using (27) of [AD4]
   (b) The maximum absolute value of the Doppler centroid across the swath is calculated
   (c) The swath overlap percentage (with nominal) is computed
5. The previous is repeated numerous times to generate histograms of the Doppler centroid and swath overlap percentage. These histograms are compared with the requirements to determine the suitability of $\mathbf{R}_{\text{aeu}}(t)$ to meet R-MIS-PER-1045. If $\mathbf{R}_{\text{aeu}}(t)$ is found not to be suitable, it is changed and steps 4 and 5 are repeated. Section 6 discusses how $\mathbf{R}_{\text{aeu}}(t)$ is modified given various input parameters.

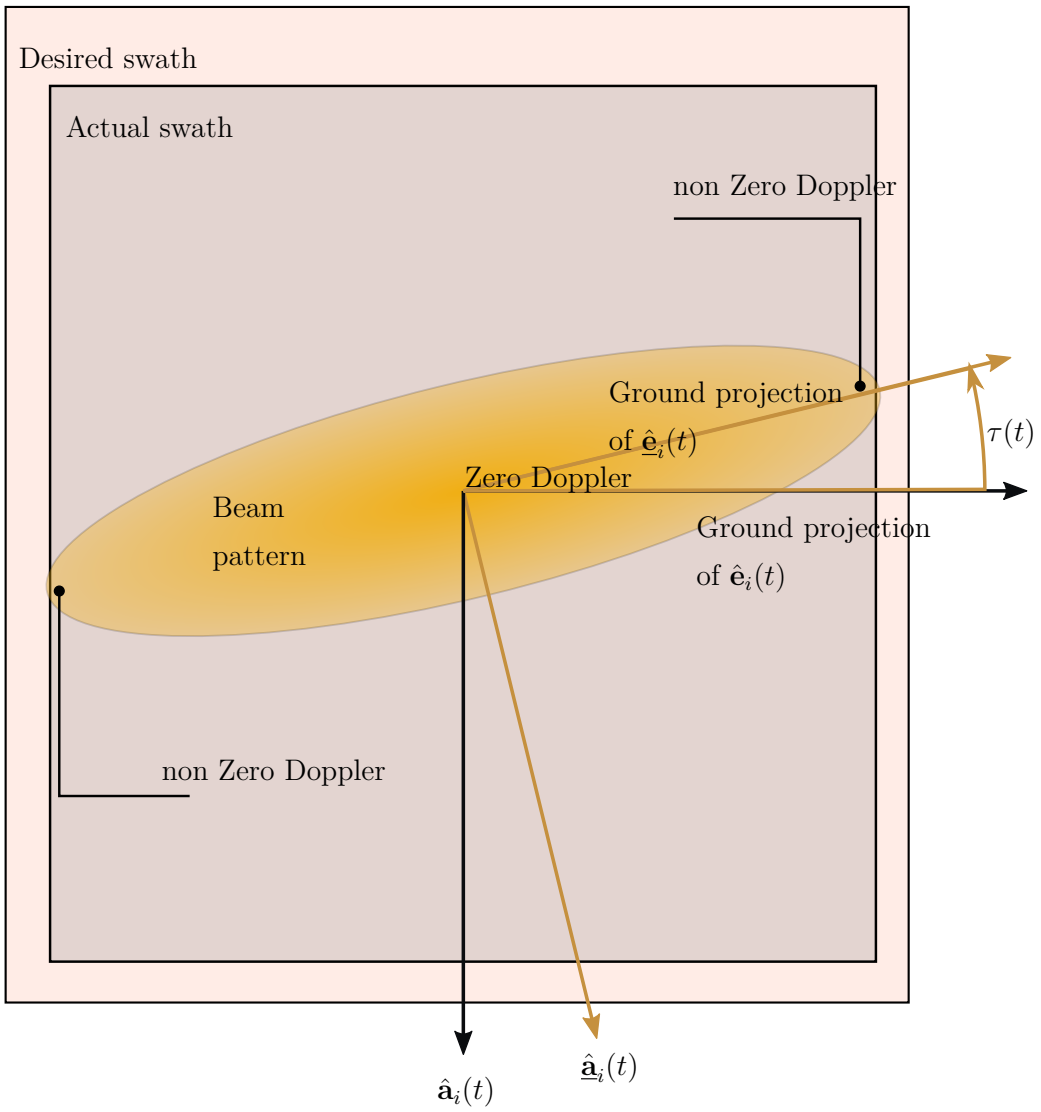

Figure 1: Illustration of effect of tilt error.

The simulation yields a set of input parameters, used to compute $\mathbf{R}_{\text{aeu}}(t)$, that lead to compliance with R-MIS-PER-1045.

6. CONSIDERED POINTING ERROR CONTRIBUTORS

Error sources are defined as the random components of the vector $\boldsymbol{\varsigma}(t)$

$$\boldsymbol{\varsigma}(t) = \begin{bmatrix} \alpha_s(t) \\ \epsilon_s(t) \\ \tau_s(t) \\ \alpha_t(t) \\ \epsilon_t(t) \\ \tau_t(t) \\ \alpha_v(t) \\ \epsilon_v(t) \\ \tau_v(t) \\ \epsilon_\delta(t) \end{bmatrix}, \tag{8}$$

where

- $\alpha_s(t)$, $\epsilon_s(t)$ and $\tau_s(t)$ are random processes with covariance matrix, $\mathbf{R}_s(t)$, reflecting errors in the ability to point the beam in a desired direction. These combine the error in star-tracker measurements, the errors induced through the mechanical steering, and errors due to thermo-elastic distortion. These errors are discussed in Section 6.1.
- $\alpha_t(t)$, $\epsilon_t(t)$ and $\tau_t(t)$ are random processes with covariance matrix, $\mathbf{R}_t(t)$, reflecting errors stemming from timing. These errors are discussed in Section 6.2.
- $\alpha_v(t)$, $\epsilon_v(t)$ and $\tau_v(t)$ are random processes with covariance matrix, $\mathbf{R}_v(t)$, reflecting satellite velocity errors. These errors are discussed in Section 6.3.
- $\epsilon_\delta(t)$ is a random process with variance, $\sigma^2_{\epsilon_\delta}(t)$, representing satellite across-track position errors. This error is discussed in Section 6.4.

Broadly speaking the last three items correspond to state vector errors (errors in relative position, time and velocity) while the first bullet corresponds to attitude errors. The next sections discuss the various error contributions and how they may be estimated.

To simplify computations, $\boldsymbol{\varsigma}(t)$ is treated as a zero-mean Gaussian random vector with a block-

diagonal covariance matrix $\mathbf{R}_{\varsigma}(t)$ given

$$\mathbf{R}_{\varsigma}(t) = \begin{bmatrix} \mathbf{R}_s(t) & & & \\ & \mathbf{R}_t(t) & & \\ & & \mathbf{R}_v(t) & \\ & & & \sigma_p^2(t) \end{bmatrix}. \tag{9}$$

The vectors,

$$\mathbf{M}_{\text{aeu}} = \begin{bmatrix} 1 & 0 & 0 & 1 & 0 & 0 & 1 & 0 & 0 & 0 \\ 0 & 1 & 0 & 0 & 1 & 0 & 0 & 1 & 0 & 1 \\ 0 & 0 & 1 & 0 & 0 & 1 & 0 & 0 & 1 & 0 \end{bmatrix}^T \tag{10}$$

can be used to compute

$$\begin{bmatrix} \alpha(t) \\ \epsilon(t) \\ \tau(t) \end{bmatrix} = \mathbf{M}_{\text{aeu}}^T \boldsymbol{\varsigma}(t). \tag{11}$$

Further,

$$\mathbf{R}_{\text{aeu}}(t) = \mathbf{M}_{\text{aeu}}^T \mathbf{R}_{\varsigma}(t) \mathbf{M}_{\text{aeu}}. \tag{12}$$

6.1. Attitude Errors

This document does not provide an assessment of the nature of the errors, $\alpha_s(t)$, $\epsilon_s(t)$ and $\tau_s(t)$. Instead, given $\mathbf{R}_{\text{rpy}}(t)$ the covariance matrix for the roll, pitch and yaw random errors, $\mathbf{R}_s(t)$ is numerically computed. Specifically, as a first iteration, the roll, pitch and yaw random errors are assumed to be zero-mean Gaussian variables with some assumed covariance matrix $\mathbf{R}_{\text{rpy}}(t)$.

The transformation from $\mathbf{R}_{\text{rpy}}(t)$ into $\mathbf{R}_s(t)$ is outlined in sections 7.6 and 5.2 of [AD4]. Note that the computed $\mathbf{R}_s(t)$ is generally not diagonal reflecting significant correlation.

As an example, if $\sigma_{\text{roll}}(t) = 4.8$ (mrad), $\sigma_{\text{pitch}}(t) = 0.4$ (mrad) and $\sigma_{\text{yaw}}(t) = 1.1$ (mrad), and

$$\mathbf{R}_{\text{rpy}}(t) = \begin{bmatrix} \sigma_{\text{roll}}^2(t) & 0 & 0 \\ 0 & \sigma_{\text{pitch}}^2(t) & 0 \\ 0 & 0 & \sigma_{\text{yaw}}(t) \end{bmatrix} \tag{13}$$

then one computes, to a single decimal place, that

$$\mathbf{R}_s(t) = \begin{bmatrix} \sigma_\alpha^2(t) & 0.0\sigma_\alpha(t)\sigma_\epsilon(t) & 0.5\sigma_\alpha(t)\sigma_\tau(t) \\ 0.0\sigma_\epsilon(t)\sigma_\alpha(t) & \sigma_\epsilon^2(t) & 0.0\sigma_\epsilon(t)\sigma_\tau(t) \\ 0.5\sigma_\tau(t)\sigma_\alpha(t) & 0.0\sigma_\tau(t)\sigma_\epsilon(t) & \sigma_\tau^2(t) \end{bmatrix}, \tag{14}$$

where $\sigma_\alpha(t) = 0.47$ (mrad), $\sigma_\epsilon(t) = 4.80$ (mrad), and $\sigma_\tau(t) = 1.07$ (mrad).

6.2. Timing Errors

Since the basis vectors of the DAEU frame, $\begin{bmatrix}\hat{\mathbf{a}}_i(t) & \hat{\mathbf{e}}_i(t) & \hat{\mathbf{u}}_i(t)\end{bmatrix}$, depend on t, any error in t induces an error in the DAEU frame.

Given a particular nominal time, t, values $\mathbf{R}_t(t)$ may be numerically computed by computing $\hat{\mathbf{a}}_i(t+\delta_t)$, $\hat{\mathbf{e}}_i(t+\delta_t)$, and $\hat{\mathbf{u}}_i(t+\delta_t)$ at values of δ_t chosen randomly from a stationary zero-mean Gaussian random process with variance $\sigma_{\delta_t}^2$. Note that this process is assumed to have an autocorrelation function longer than the synthetic aperture time. For each δ_t, $\begin{bmatrix}\hat{\mathbf{a}}_i(t+\delta_t) & \hat{\mathbf{e}}_i(t+\delta_t) & \hat{\mathbf{u}}_i(t+\delta_t)\end{bmatrix}$ can be compared to $\begin{bmatrix}\hat{\mathbf{a}}_i(t) & \hat{\mathbf{e}}_i(t) & \hat{\mathbf{u}}_i(t)\end{bmatrix}$ and values for $\epsilon(t)$, $\alpha(t)$ and $\tau(t)$ can be computed by inverting Equation (27) in [AD4].

After repeated application, realizations of these random variables may be used to estimate $\mathbf{R}_t(t)$.

6.3. Satellite Velocity Errors

If the satellite velocity vector is in error, then the computed look direction will not point to zero-Doppler. Since the guidance laws for the satellite depend on the Keplerian orbit elements and the orbit angle, (or time after the ascending node), it may be that the actual satellite velocity vector varies from this nominal value by

$$\boldsymbol{\delta}_{\mathbf{v}}(t) = \begin{bmatrix} \delta_{v_x}(t) \\ \delta_{v_y}(t) \\ \delta_{v_z}(t) \end{bmatrix} \tag{15}$$

where each vector element is modelled as a zero-mean Gaussian random process with covariance matrix $\mathbf{R}_{\text{vel}}(t)$. Note that although not necessarily a stationary process, $\mathcal{E}\{\boldsymbol{\delta}_{\mathbf{v}}(t_1)\boldsymbol{\delta}_{\mathbf{v}}^T(t_2)\}$ is assumed to remain constant for $t_2 - t_1$ less than the synthetic aperture time.

To compute the impact of these errors on pointing, the DAEU frame is computed using (45) by using a satellite velocity given by $\dot{\mathbf{x}}_i(t)+\boldsymbol{\delta}_{\mathbf{v}}(t)$ for various realizations of $\boldsymbol{\delta}_{\mathbf{v}}(t)$. The required angles $\epsilon(t)$, $\alpha(t)$ and $\tau(t)$ to rotate this frame into the AAEU frame (the solution of (45) without $\boldsymbol{\delta}_{\mathbf{v}}(t)$) are then computed and used to estimate $\mathbf{R}_v(t)$.

6.4. Across-Track Position Errors

According to [AP-ECSS], the APE specification can, "refer to an inertial frame or to an Earth-oriented reference frame. In the latter case, the effect of orbit knowledge erros can be included." In this document, the effects of imperfect knowledge of orbit and terrain shall be included in the specification of the elevation APE.

Attitude control aims to steer the spacecraft so that the radar antenna aligns with the DEAU frame and assumes an ideal Keplerian orbit and a perfectly well known surface height.

This section examines the first-order impacts of errors in the orbit and surface height. Strictly speaking, errors in satellite position or terrain height are not pointing errors. Instead, the effects of these errors can be related to equivalent pointing errors. This allows simulation simplification.

The error model assumes that the offset of the satellite from its ideal position, $\boldsymbol{\delta}_{\mathbf{p}}(t)$, remains constant throughout the SAR acquisition. Furthermore, the model assumes no component of $\boldsymbol{\delta}_{\mathbf{p}}(t)$ in the direction of motion of the SAR satellite, since, through its motion, the satellite will simply image from such a shifted location at a slightly different time – this is why $\alpha_\delta(t) = \tau_\delta(t) = 0$.

Specifically, two effects arise from a satellite across-track position error. First, because the look direction will be commanded assuming the ideal position, the ground intercept of the boresight will change as illustrated in Figure 2. These shifts can cause non-compliance with R-MIS-PER-1045.

Second, because the echo window timing will be commanded according to the ideal position, the ground swath will change as illustrated in Figure 3. As the figures illustrate, not only is the projection of the echo window shifted relative to ideal, but the boresight is also shifted away from the center of the echo window resulting in lower than expected SNR. This shift in the ground swath can cause non-compliance with R-MIS-PER-XXXX.

6.4.1. Elevation Angle Error due to Ground Intercept of Boresight

To model error in the satellite position, we make use of the following approximation

$$\begin{aligned}\hat{\mathbf{u}}'_p(t) = \frac{\mathbf{r}_0(t) + \boldsymbol{\zeta}(t)}{|\mathbf{r}_0(t) + \boldsymbol{\zeta}(t)|} &\approx \hat{\mathbf{r}}_0(t) + \frac{\mathbf{I} - \hat{\mathbf{r}}_0(t)\hat{\mathbf{r}}_0^T(t)}{|\mathbf{r}_0(t)|}\boldsymbol{\zeta}(t) \\ &= \hat{\mathbf{u}}_p(t) + \frac{\boldsymbol{\zeta}_\perp(t)}{r_0(t)}\end{aligned} \tag{16}$$

where $\boldsymbol{\zeta}_\perp(t)$ is the component of $\boldsymbol{\zeta}(t)$ that is perpendicular to $\hat{\mathbf{u}}_p(t)$; $\mathbf{r}_0(t)$ is the vector from the ideal satellite position to the point on the planet surface in the boresight direction, see figure 2; and $r_0(t) = |\mathbf{r}_0(t)|$. Clearly, from figure 2, $\boldsymbol{\delta}_{\mathbf{p}_\perp}(t) = \boldsymbol{\zeta}_\perp(t)$, where $\boldsymbol{\delta}_{\mathbf{p}_\perp}(t)$ is the component of $\boldsymbol{\delta}_{\mathbf{p}}(t)$

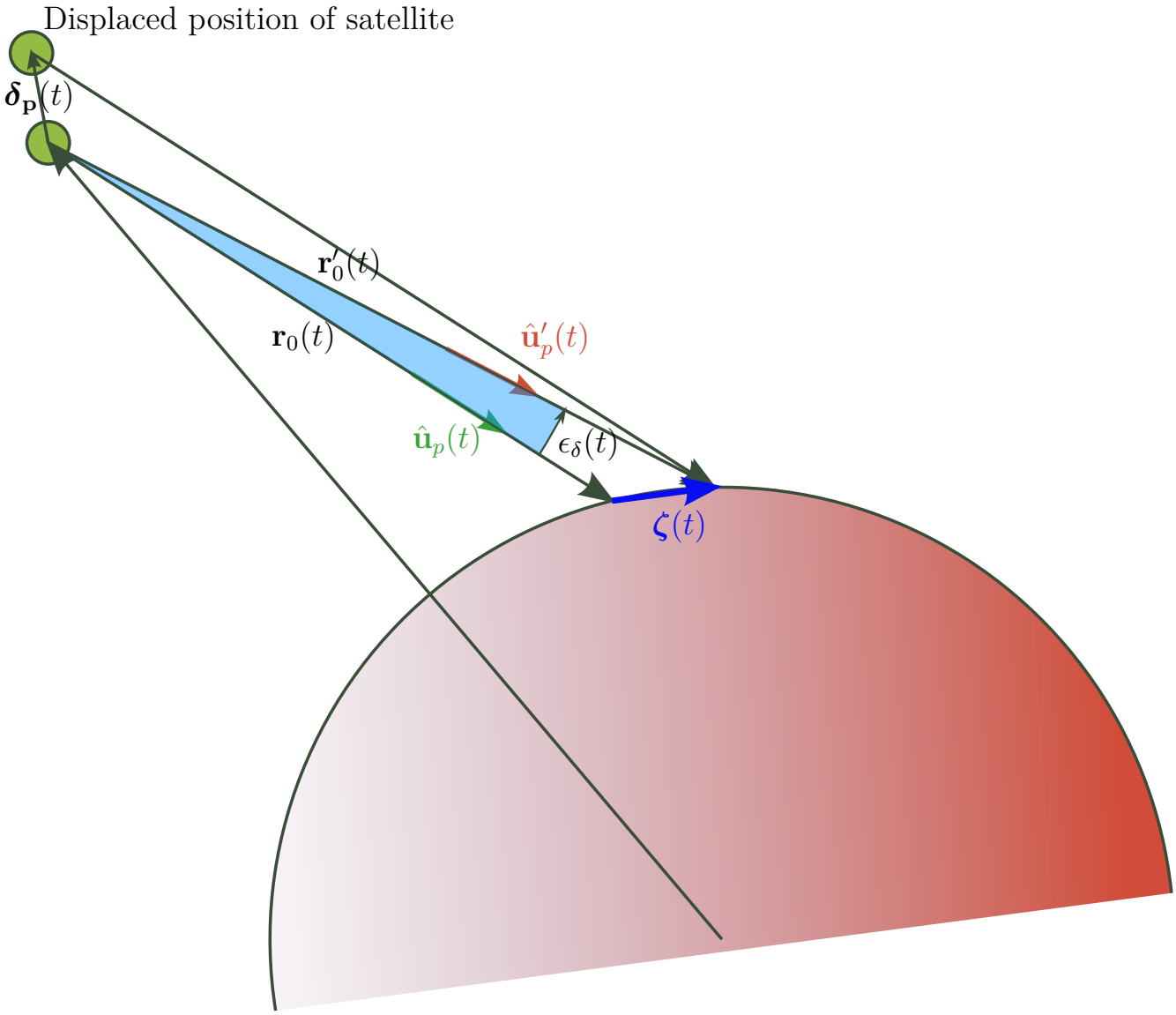

Figure 2: Orbit error.

that is perpendicular to $\hat{\mathbf{u}}_p(t)$; thus,

$$\hat{\mathbf{u}}_p'(t) \approx \hat{\mathbf{u}}_p(t) + \frac{\boldsymbol{\delta}_{\mathbf{p}_\perp}(t)}{r_0(t)} \tag{17}$$

By taking the inner product of both sides with $-\hat{\mathbf{x}}_p(t)$, one finds, from (43), that

$$v'(t) = v(t) - \frac{\hat{\mathbf{x}}_p^T(t)\boldsymbol{\delta}_{\mathbf{p}_\perp}(t)}{r_0(t)}, \tag{18}$$

and since $v'(t) = \cos[\theta_d(t) + \epsilon_\delta(t)] \approx \cos\theta_d(t) - \epsilon_\delta(t)\sin\theta_d(t)$, for some desired off-nadir angle,

$\theta_d(t)$, and some off-nadir angle error $\epsilon_\delta(t)$, one sees that

$$v'(t) - v(t) \approx \cos[\theta_d(t) + \epsilon_\delta(t)] - \cos\theta_d(t) \approx -\epsilon_\delta(t)\sin\theta_d(t) \tag{19}$$

Also,

$$-\frac{\hat{\mathbf{x}}_p^T(t)\boldsymbol{\delta}_{\mathbf{p}_\perp}(t)}{r_0(t)} = \frac{|\boldsymbol{\delta}_{\mathbf{p}_\perp}(t)|\cos[\theta_d(t) \pm \pi/2]}{r_0(t)} = \mp\frac{|\boldsymbol{\delta}_{\mathbf{p}_\perp}(t)|\sin\theta_d(t)}{r_0(t)}, \tag{20}$$

where the sign depends on whether $\hat{\mathbf{u}}_p^T(t)\boldsymbol{\delta}_{\mathbf{p}}(t)$ is positive or negative. By equating the last two equations, one finds that

$$\epsilon_\delta(t) = \pm\frac{|\boldsymbol{\delta}_{\mathbf{p}_\perp}(t)|}{r_0(t)}. \tag{21}$$

This document assumes that across-track deviations of the satellite from its nominal position at time, t, are described by a two-dimensional Gaussian (around the orbit tube) random process, with mean value zero and equal variances, $\sigma_P^2(t)$ in both the line-of-sight and perpendicular to the line of sight directions. The previous analysis shows that the error introduced in the elevation angle may be approximated as a zero-mean Gaussian with standard deviation

$$\sigma_{\epsilon_\delta}^2(t) = \frac{\sigma_p^2(t)}{r_0^2(t)}. \tag{22}$$

6.4.2. Ground Swath Placement Error

The effective ground swath displacement due to satellite position error is illustrated in Figures 3 where it can be seen that the shift is approximately given by

$$s_g(t) = \frac{\boldsymbol{\delta}_{\mathbf{p}}^T(t)\hat{\mathbf{r}}_0(t)}{\sin\theta_i(t)}, \tag{23}$$

where $\theta_i(t)$ is the desired incidence angle.

This document assumes statistical independence between the parallel and perpendicular components of the satellite position error; thus, respective contributions to swath placement and elevation angle are also considered statistically independent.

One may therefore define the Gaussian random process $W(t) = \boldsymbol{\delta}_{\mathbf{p}}^T(t)\hat{\mathbf{r}}_0(t) \sim N(0, \sigma_p^2(t))$. Now, given some swath width, S_w, R-MIS-PER-XXXX requires that

$$\mathrm{P}\left(\left|\frac{W(t)}{\sin\theta_i(t)}\right| \leq \frac{S_w}{15}\right) = \mathrm{P}\left(|W(t)| \leq \frac{S_w\sin\theta_i(t)}{15}\right) = 0.95 \tag{24}$$

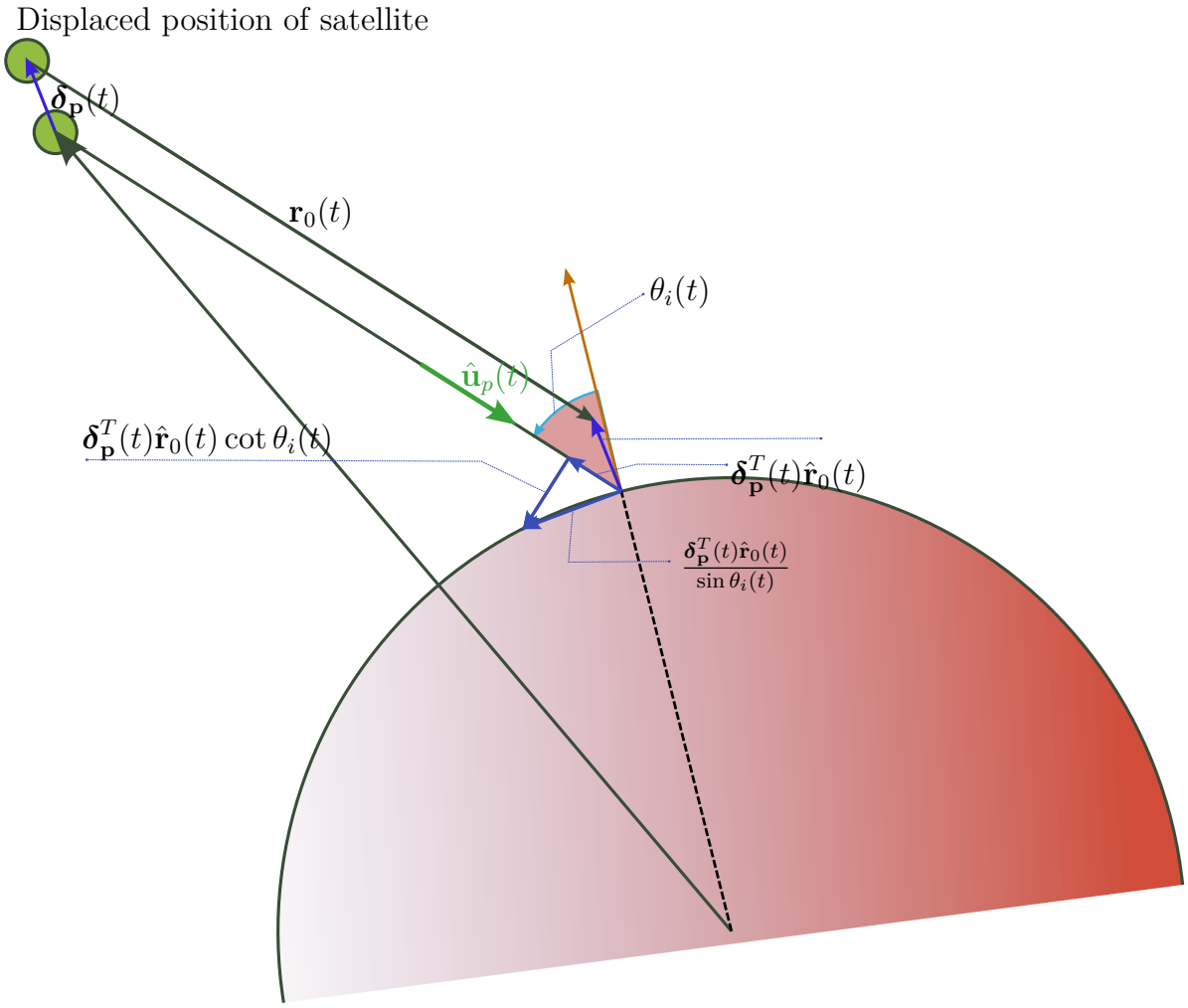

Figure 3: Echo window placement error due to orbit error.

which, for $W(t) \sim N(0, \sigma_p^2(t))$ yields the constraint that

$$2\sigma_p(t) \leq \frac{S_w \sin\theta_i(t)}{15} \tag{25}$$

The above expression provides a constraint on the satellite positional error that exists independently of the pointing errors. Specifically,

- a smallest swath with of 20 km from R-MIS-PER-0489 [AD6], and
- a maximum incidence angle of 40° from R-MIS-PER-0024 [AD6],

mean that $\sigma_p(t) \leq 430$m.

6.4.3. Summary of Satellite Position Error Contributions

This section demonstrates that satellite position errors manifest in angular elevation errors and errors in placement of the ground swath.

Because the intercept of the boresight with the ground occurs at a position other than that expected from the DAEU frame, this effect can be considered a pointing error. In other words, if the satellite is assumed to be at the ideal position, then the AAEU frame corresponds to a boresight defined by (21). This section shows that this contributor to elevation error depends on the component of the satellite position error (or terrain position error) that is **perpendicular** to the line of sight vector.

The error in the placement of the swath does not relate to the look direction. However, due to improper timing resulting from spatial displacements of the satellite or terrain from expected, the actual imaged ground swath may cause non-compliance with R-MIS-PER-XXXX. This section shows that the swath placement error depends on the component of satellite position error (or terrain position error) that is **parallel** to the line of sight vector. Further, without the need for simulation, the section shows that the ground swath placement requirement implies that the standard deviation of the orbit tube must satisfy $\sigma_p(t) \leq 430\text{m}$.

7. POINTING ERROR SIMULATION

This section applies the method of Section 5 to generate concrete tolerances for Envision. Simulations are generated with custom Python with code.

In the first iteration of the simulation, the parameters of time-dependent random variables are assumed constant. Also, $\mathbf{R}_{\text{vel}}(t)$ and $\mathbf{R}_{\text{rpy}}(t)$ are assumed to be diagonal matrices.

The following data are used in the simulation

7.1. Parameters

Parameter	Value
Orbit File	EnVision_ALT_T4_2032_SouthVOI.oem
$\begin{bmatrix}\sigma_{\text{roll}}(t) & \sigma_{\text{pitch}}(t) & \sigma_{\text{yaw}}(t)\end{bmatrix}$	$\begin{bmatrix}4.8 & 0.4 & 1.1\end{bmatrix}$ (mrad)
σ_{δ_t}	5 (s)
$\begin{bmatrix}\sigma_{v_x}(t) & \sigma_{v_y}(t) & \sigma_{v_z}(t)\end{bmatrix}$	$\begin{bmatrix}0.2 & 0.2 & 0.2\end{bmatrix}$ (m/s)
$\sigma_p(t)$	600 (m)
Venus geometry	Spherical (r=6051878 m)
Venus mass	4.867e+24 (Kg)
Venus rotation rate	-2.99234e-07 (rad/s)
SAR off-nadir angle	30 (deg)
ϵ_0	14.28 (deg)
Antenna length azimuth	6.0 (m)
Antenna length elevation	0.6 (m)

Table 2: Parameters used for pointing tolerance simulation

7.2. Results

Figures 4 and 5 show how, with the chosen parameters of Table 2, the requiremens for R-MIS-PER-1045 are met about 95% of the time. Figure 4 indicates that the swath overlap is less than 14/15 for only 4.92% of repeated trials. Figure 5 indicates that the Doppler centroid exceeds 1/15

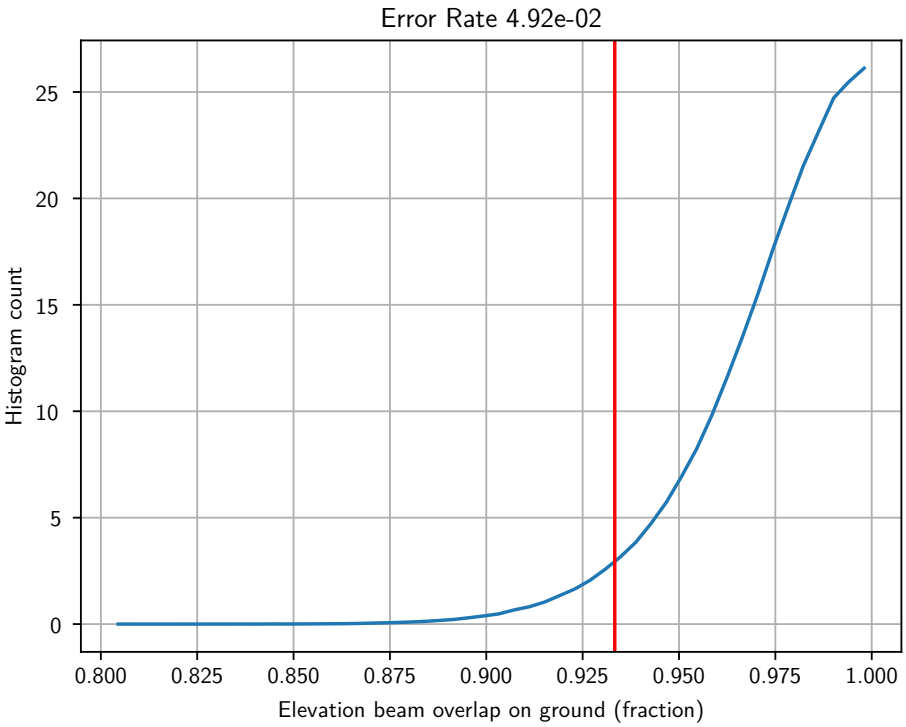

Figure 4: Example of swath overlap histogram. The red line indicates the 95% threshold of R-MIS-PER-1045.

of the Doppler bandwidth for only 4.75% of repeated trials.

Figure 6 shows how pitch and yaw standard deviations impact on the percentage of trials that violate the 1/15 of the Doppler bandwidth requirement. The figure shows that the pitch and yaw errors act independently from the roll error with respect to satifying the Doppler centroid component of R-MIS-PER-1045. Figure 6a has been computed under the condition that $\sigma_{\text{roll}} = 4.8$ (mrad); thus, the choice of values for $\sigma_{\text{pitch}}, \sigma_{\text{yaw}}$ in Table 2 can be read directly from the graph.

Figure 7 shows how, over different orbit positions and with the parameters of Table 2, the requirements for R-MIS-PER-1045 are met at a rate slightly greater than 95% of the time. The cyclical nature of the swath error plot illustrates the orbit-related range dependence of the satellite position error contribution to $\epsilon(t)$, see (21).

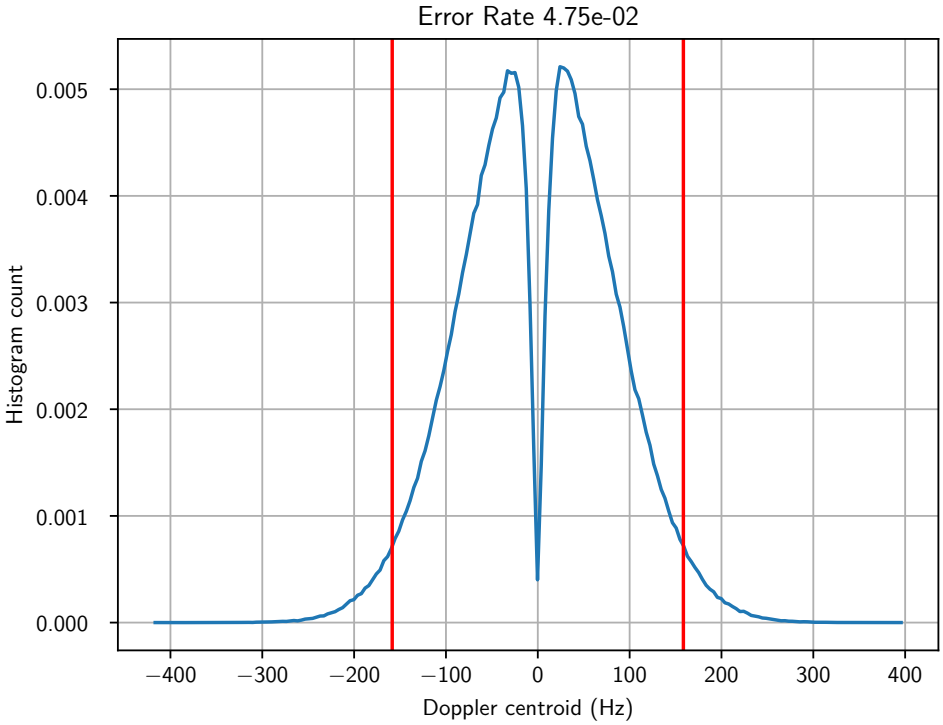

Figure 5: Example of Doppler centroid histogram. The red lines indicate the 95% threshold of R-MIS-PER-1045.

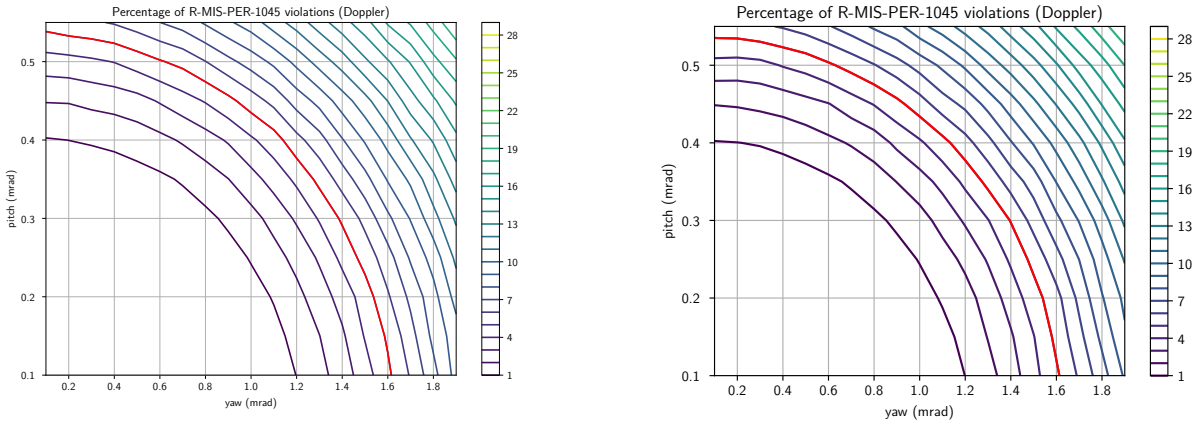

(a) Roll standard deviation: 4.8 (mrad).

(b) Roll standard deviation: 5.8 (mrad).

Figure 6: Impact of pitch and yaw standard deviations on the percentage of violations of the Doppler component of R-MIS-PER-1045. The figures demonstrate independence from the roll error. The red lines indicates the 5% threshold, while other lines are increments of 1%.

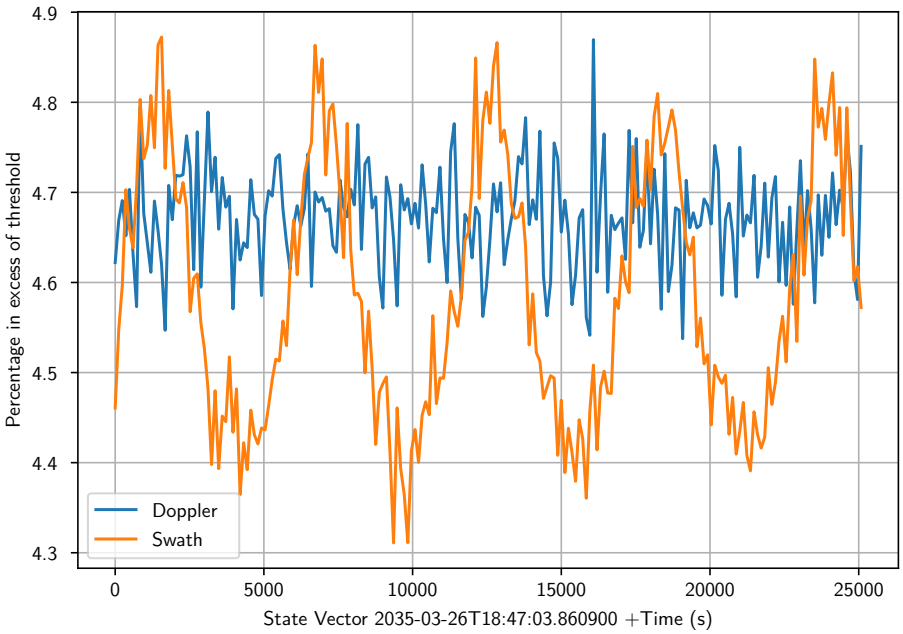

Figure 7: Percentage of violations of R-MIS-PER-1045 over time.

7.3. Summary

Simulations indicate that the values listed in Table 2 allow compliance with R-MIS-PER-1045. Figure 6 indicates that the standard deviation of pitch and yaw error should be kept below 0.4 (mrad) and 1.1 (mrad), respectively.

A. ORBIT ELLIPSE FRAME SATELLITE TRACK

In the OE reference frame, [AD4], a satellite track may be written as

$$\mathbf{x}_o(t) = \alpha_{o_n}(t)\mathbf{n}_o(t) + \alpha_{o_t}(t)\mathbf{t}_o(t). \tag{26}$$

According to Figure 9, the coefficients are given by

$$\alpha_{o_n}(t) = -R(t)\cos\gamma(t) \tag{27}$$
$$\alpha_{o_t}(t) = R(t)\sin\gamma(t) \tag{28}$$

A.1. Some useful products

In order to facilitate further calculations, note that $\mathbf{I}_2\mathbf{t}_o(t) = \mathbf{t}_o(t)$ and $\mathbf{I}_2\mathbf{n}_o(t) = \mathbf{n}_o(t)$. These relations stem from the fact that the vectors lie in the orbit plane and thus have no $\hat{\mathbf{k}}_o$ component.

According to [AD4],

$$\begin{aligned}\mathbf{t}_i^T(t)\mathbf{Q}_2\mathbf{n}_i(t) &= [\mathbf{M}_i(\theta_i)\mathbf{t}_o(t)]^T\mathbf{Q}_2\mathbf{M}_i(\theta_i)\mathbf{n}_o(t)\\ &= \mathbf{t}_o^T(t)\mathbf{M}_i^T(\theta_i)\mathbf{Q}_2\mathbf{M}_i(\theta_i)\mathbf{n}_o(t).\end{aligned} \tag{29}$$

By direct computation, one finds that

$$\mathbf{I}_2^T\mathbf{M}_i^T(\theta_i)\mathbf{Q}_2\mathbf{M}_i(\theta_i)\mathbf{I}_2 = \cos\theta_i\mathbf{Q}_2. \tag{30}$$

Therefore,

$$\begin{aligned}\mathbf{t}_i^T(t)\mathbf{Q}_2\mathbf{n}_i(t) &= \cos\theta_i\mathbf{t}_o^T(t)\mathbf{Q}_2\mathbf{n}_o(t)\\ &= \cos\theta_i,\end{aligned} \tag{31}$$

where the above follows from the following argument: according to Figure 8, one sees that

$$\begin{aligned}\mathbf{t}_o^T(t)\mathbf{Q}_2\mathbf{n}_o(t) &= n_{o_y}t_{o_x} - n_{o_x}t_{o_y}\\ &= \cos\delta\sin\left(\frac{\pi}{2}-\delta\right) + \sin\delta\cos\left(\frac{\pi}{2}-\delta\right)\\ &= \sin^2\delta + \cos^2\delta\\ &= 1\end{aligned} \tag{32}$$

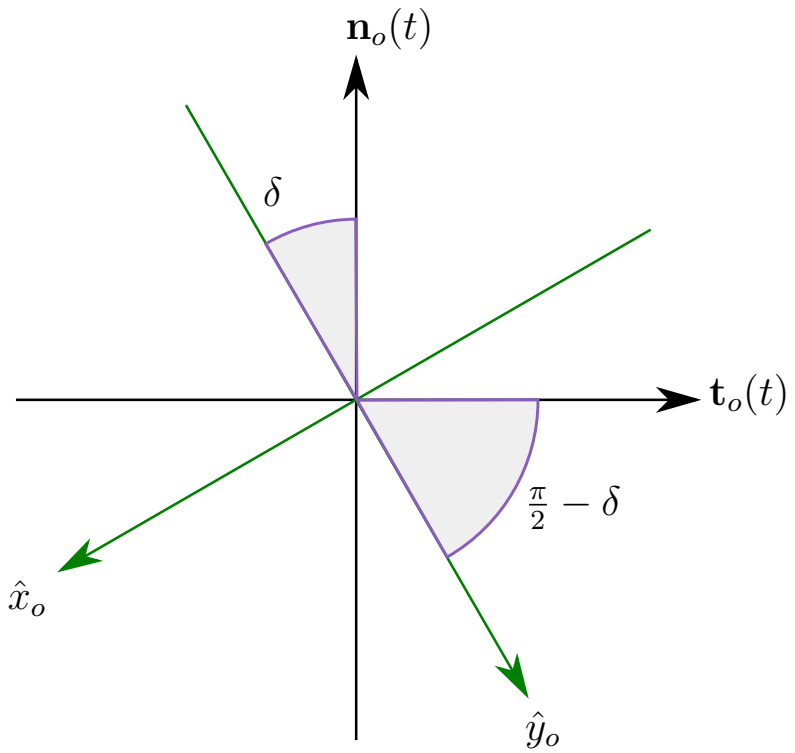

Figure 8: Projection of the tangential and normal vecctors onto the orbital inertial axes.

From similar arguments

$$\mathbf{c}_i^T(t)\mathbf{Q}_2\mathbf{n}_i(t) = -n_{o_y}(t)\sin\theta_i = \cos[\beta(t) - \gamma(t)]\sin\theta_i \tag{33}$$
$$\mathbf{c}_i^T(t)\mathbf{Q}_2\mathbf{t}_i(t) = -t_{o_y}(t)\sin\theta_i = \sin[\beta(t) - \gamma(t)]\sin\theta_i \tag{34}$$
$$\mathbf{n}_i^T(t)\mathbf{Q}_2\mathbf{t}_i(t) = -\cos\theta_i \tag{35}$$
$$\mathbf{t}_i^T(t)\mathbf{Q}_2\mathbf{t}_i(t) = 0 \tag{36}$$
$$\mathbf{n}_i^T(t)\mathbf{Q}_2\mathbf{n}_i(t) = 0 \tag{37}$$
$$\mathbf{c}_i^T(t)\mathbf{Q}_2\mathbf{c}_i(t) = 0, \tag{38}$$
$$\tag{39}$$

where

$$n_{o_y}(t) = -\cos[\beta(t) - \gamma(t)] \tag{40}$$
$$t_{o_y}(t) = -\sin[\beta(t) - \gamma(t)] \tag{41}$$

follows from Figure 9.

B. CONDITIONS FOR ZERO-DOPPLER STEERING

With the assumption that the look vector of the system in the PCR frame (see [AD4]) is given by $\hat{\mathbf{u}}_p(t)$, the following two requirements ensure zero-Doppler steering

$$\hat{\mathbf{u}}_p^T(t)\dot{\mathbf{x}}_p(t) = 0, \tag{42}$$

$$-\hat{\mathbf{u}}_p^T(t)\hat{\mathbf{x}}_p(t) = v(t). \tag{43}$$

The first relation implies that, from the point of view of an individual standing on the planet surface, the look vector is always perpendicular to the satellite track. With this condition, for any point on the surface, the satellite will have a minimum range to that point when the vector from the satellite to the point is perpendicular to the satellite track.

The second condition varies the across-track off-nadir (relative to centre of the planet, not the surface) angle. The desired $v(t)$ can be adjusted to point the boresight such that it is centered on a swath parallel to the ground track of the satellite, or it can be chosen to point the boresight to the centre of a swath that minimizes changes to the range echo window timing. The second option is of particular interest when the planet is highly ellipsoidal or when the satellite orbit has high eccentricity. Indeed some EO SAR satellites apply the so-called roll-steering law for just this purpose. The negative sign arises from the fact that $\mathbf{x}_p(t)$ is the vector upwards, from the planet center to the satellite, while the satellite beam points downwards towards the surface.

B.1. Transformation of zero-Doppler Conditions from PCI to PCR

In this section the zero-Doppler requirement defined for the PCR frame is translated into the PCI frame. This is because the attitude of the satellite is controlled with reference to the PCI frame or with respect to $\mathbf{t}_i(t), \mathbf{c}_i(t), \mathbf{n}_i(t)$.

By using the reference frame transformations in [AD4], the zero-Doppler conditions transform from the PCR system into the PCI system as

$$\begin{aligned}
\hat{\mathbf{u}}_p^T(t)\dot{\mathbf{x}}_p(t) &= 0 \\
\left[\mathbf{M}(t)\hat{\mathbf{u}}_i(t)\right]^T \left[\dot{\mathbf{M}}(t)\mathbf{x}_i(t) + \mathbf{M}(t)\dot{\mathbf{x}}_i(t)\right] &= 0 \\
\hat{\mathbf{u}}_i^T(t) \left[\mathbf{M}^T(t)\dot{\mathbf{M}}(t)\mathbf{x}_i(t) + \mathbf{M}^T(t)\mathbf{M}(t)\dot{\mathbf{x}}_i(t)\right] &= 0 \\
\hat{\mathbf{u}}_i^T(t) \left[\omega_p \mathbf{Q}_2 \mathbf{x}_i(t) + \dot{\mathbf{x}}_i(t)\right] &= 0,
\end{aligned} \tag{44}$$

and

$$\begin{aligned}
-v(t) &= \hat{\mathbf{u}}_p^T(t)\hat{\mathbf{x}}_p(t) \\
&= \left[\mathbf{M}(t)\hat{\mathbf{u}}_i(t)\right]^T \mathbf{M}(t)\hat{\mathbf{x}}_i(t) \\
&= \hat{\mathbf{u}}_i^T(t)\hat{\mathbf{x}}_i(t)
\end{aligned} \tag{45}$$

For use later on, represent the look vector as

$$\hat{\mathbf{u}}_i(t) = u_{i_t}(t)\mathbf{t}_i(t) + u_{i_c}(t)\mathbf{c}_i(t) + u_{i_n}(t)\mathbf{n}_i(t). \tag{46}$$

Now, since

$$\mathbf{x}_i(t) = \alpha_{o_n}(t)\mathbf{n}_i(t) + \alpha_{o_t}(t)\mathbf{t}_i(t), \tag{47}$$

the left side of the last line of (45) may be written as

$$\begin{aligned}
&[u_{i_t}(t)\mathbf{t}_i(t) + u_{i_c}(t)\mathbf{c}_i(t) + u_{i_n}(t)\mathbf{n}_i(t)]^T[\omega_p\mathbf{Q}_2[\alpha_{o_n}(t)\mathbf{n}_i(t) + \alpha_{o_t}(t)\mathbf{t}_i(t)] + v_s(t)\mathbf{t}_i(t)] \\
&\quad = \omega_p u_{i_t}(t)\alpha_{o_n}(t)\mathbf{t}_i^T(t)\mathbf{Q}_2\mathbf{n}_i(t) + \omega_p u_{i_n}(t)\alpha_{o_t}(t)\mathbf{n}_i^T(t)\mathbf{Q}_2\mathbf{t}_i(t) \\
&\quad + \omega_p u_{i_c}(t)\alpha_{o_n}(t)\mathbf{c}_i^T(t)\mathbf{Q}_2\mathbf{n}_i(t) + \omega_p u_{i_c}(t)\alpha_{o_t}(t)\mathbf{c}_i^T(t)\mathbf{Q}_2\mathbf{t}_i(t) \\
&\quad + v_s(t)u_{i_t}(t) \\
&\quad = \omega_p \cos\theta_i \left[u_{i_t}(t)\alpha_{o_n}(t) - u_{i_n}(t)\alpha_{o_t}(t)\right] \\
&\quad - \omega_p u_{i_c}(t)\sin\theta_i \left[\alpha_{o_n}(t)n_{o_y}(t) + \alpha_{o_t}(t)t_{o_y}(t)\right] \\
&\quad + v_s(t)u_{i_t}(t).
\end{aligned} \tag{48}$$

With the relations

$$\alpha_{o_n}(t) = -R(t)\cos\gamma(t) \tag{49}$$

$$\alpha_{o_t}(t) = R(t)\sin\gamma(t), \tag{50}$$

and the expressions in (40) and (41), one finds that

$$\begin{aligned}
&u_{i_t}(t)\left[-\omega_p R(t)\cos\theta_i\cos\gamma(t) + v_s(t)\right] \\
&u_{i_c}(t)\left[-\omega_p R(t)\sin\theta_i\cos\beta(t)\right] \\
&u_{i_n}(t)\left[-\omega_p R(t)\cos\theta_i\sin\gamma(t)\right] = 0,
\end{aligned} \tag{51}$$

which may be written as

$$\hat{\mathbf{u}}_i^T(t)\begin{bmatrix} D(t) - \cos\theta_i\cos\gamma(t) \\ -\sin\theta_i\cos\beta(t) \\ -\cos\theta_i\sin\gamma(t) \end{bmatrix} = 0, \tag{52}$$

where

$$D(t) = \frac{v_s(t)}{\omega_p R(t)} = \frac{\omega_o(t)}{\omega_p}. \tag{53}$$

The additional constraint for the depression angle then leads to following expression

$$\hat{\mathbf{u}}_i^T(t)\begin{bmatrix} D(t)-\cos\theta_i\cos\gamma(t) & -\sin\gamma(t) \\ -\sin\theta_i\cos\beta(t) & 0 \\ -\cos\theta_i\sin\gamma(t) & \cos\gamma(t) \end{bmatrix} = \begin{bmatrix} 0 & v(t) \end{bmatrix} \tag{54}$$
$$\text{Subject to } \hat{\mathbf{u}}_i^T(t)\hat{\mathbf{u}}_i(t) = 1$$

B.2. Solving for the zero-Doppler look vector

The constraint in (54) needs to be inverted to find an expression for $\hat{\mathbf{u}}_i(t)$. Let us write that

$$\mathbf{v}_1^T(t) = \begin{bmatrix} D(t)-\cos\theta_i\cos\gamma(t) & -\sin\theta_i\cos\beta(t) & -\cos\theta_i\sin\gamma(t) \end{bmatrix} \tag{55}$$
$$\mathbf{v}_2^T(t) = \begin{bmatrix} -\sin\gamma(t) & 0 & \cos\gamma(t) \end{bmatrix}. \tag{56}$$

The task at hand is to find the solution to

$$\hat{\mathbf{u}}_i^T(t)\mathbf{V}(t) = \begin{bmatrix} 0 & v(t) \end{bmatrix}, \tag{57}$$

subject to $\hat{\mathbf{u}}_i^T(t)\hat{\mathbf{u}}_i(t) = 1$, and where $\mathbf{V}(t) = \begin{bmatrix} \mathbf{v}_1(t) & \mathbf{v}_2(t) \end{bmatrix}$.

Without the constraint that $\hat{\mathbf{u}}_i(t)$ is a unit vector, the system of equations in (57) is underdetermined. That is, while $\hat{\mathbf{u}}_i(t)$ is a 3-element vector, there are only two vectors in $\mathbf{V}(t)$, thus only two constraints. To find a solution, we suppose that there exists a vector $\mathbf{w}(t)$ which is perpendicular to both $\mathbf{v}_1(t)$ and $\mathbf{v}_2(t)$. This vector defines the null space of $\mathbf{V}(t)$. Now suppose we have a solution, $\hat{\mathbf{u}}_0(t)$ such that

$$\hat{\mathbf{u}}_0^T(t)\mathbf{V}(t) = \begin{bmatrix} 0 & v(t) \end{bmatrix}. \tag{58}$$

It then follows that, for all $s(t)$, $\hat{\mathbf{u}}(t) = \hat{\mathbf{u}}_0(t) + s(t)\mathbf{w}(t)$ also satisfies (58). Given knowledge of $\hat{\mathbf{u}}_0(t)$ and $\mathbf{w}(t)$, one can then find the specific value(s) of $s(t)$ such that $\hat{\mathbf{u}}^T(t)\hat{\mathbf{u}}(t) = 1$.

By inspection, one sees that a candidate for $\hat{\mathbf{u}}_0(t)$ is

$$\hat{\mathbf{u}}_0(t) = v(t)\begin{bmatrix} -\sin\gamma(t) \\ -\frac{D(t)\sin\gamma(t)}{\sin\theta_i\cos\beta(t)} \\ \cos\gamma(t) \end{bmatrix}. \tag{59}$$

As well, the vector $\mathbf{w}(t)$ may be computed as $\mathbf{w}(t) = \mathbf{v}_2(t) \times \mathbf{v}_1(t)$, which evaluates to

$$\mathbf{w}(t) = \begin{bmatrix} \cos\gamma(t)\cos\beta(t)\sin\theta_i \\ D(t)\cos\gamma(t) - \cos\theta_i \\ \sin\gamma(t)\cos\beta(t)\sin\theta_i \end{bmatrix}. \tag{60}$$

The final solution is thus

$$\hat{\mathbf{u}}_i(t) = v(t) \begin{bmatrix} -\sin\gamma(t) \\ -\frac{D(t)\sin\gamma(t)}{\sin\theta_i\cos\beta(t)} \\ \cos\gamma(t) \end{bmatrix} + s(t) \begin{bmatrix} \cos\gamma(t)\cos\beta(t)\sin\theta_i \\ D(t)\cos\gamma(t) - \cos\theta_i \\ \sin\gamma(t)\cos\beta(t)\sin\theta_i \end{bmatrix} \tag{61}$$

where $s(t)$ is chosen so that $\hat{\mathbf{u}}_i^T(t)\hat{\mathbf{u}}_i(t) = 1$.

B.2.1. Specific solution for the zero-Doppler look vector in the PCI frame

Rewrite the solution as

$$\hat{\mathbf{u}}_i(t) = \mathbf{e}_1(t) + s(t)\mathbf{e}_2(t), \tag{62}$$

where

$$\mathbf{e}_1(t) = v(t) \begin{bmatrix} -\sin\gamma(t) \\ -\frac{D(t)\sin\gamma(t)}{\sin\theta_i\cos\beta(t)} \\ \cos\gamma(t) \end{bmatrix} \tag{63}$$

and

$$\mathbf{e}_2(t) = \begin{bmatrix} \cos\gamma(t)\cos\beta(t)\sin\theta_i \\ D(t)\cos\gamma(t) - \cos\theta_i \\ \sin\gamma(t)\cos\beta(t)\sin\theta_i \end{bmatrix}. \tag{64}$$

With this notation, one arrives at the condition that

$$s^2(t)|\mathbf{e}_2(t)|^2 + 2s(t)\mathbf{e}_1^T(t)\mathbf{e}_2(t) + |\mathbf{e}_1(t)|^2 = 1, \tag{65}$$

which means that $s(t)$ is the solution of

$$s(t) = \frac{-\mathbf{e}_1^T(t)\mathbf{e}_2(t) \pm \sqrt{\left[\mathbf{e}_1^T(t)\mathbf{e}_2(t)\right]^2 - |\mathbf{e}_2(t)|^2\left[|\mathbf{e}_1(t)|^2 - 1\right]}}{|\mathbf{e}_2(t)|^2} \tag{66}$$

By direct calculation

$$\mathbf{e}_1^T(t)\mathbf{e}_1(t) = v^2(t) + \frac{v^2(t)D^2(t)\sin^2\gamma(t)}{\sin^2\theta_i\cos^2\beta(t)} \tag{67}$$

$$\mathbf{e}_1^T(t)\mathbf{e}_2(t) = -\frac{v(t)D(t)\sin\gamma(t)}{\sin\theta_i\cos\beta(t)}F(t) \tag{68}$$

$$\mathbf{e}_2^T(t)\mathbf{e}_2(t) = \sin^2\theta_i\cos^2\beta(t) + F^2(t), \tag{69}$$

where

$$F(t) = D(t)\cos\gamma(t) - \cos\theta_i \tag{70}$$

The computed solution is,

$$\begin{aligned} s(t) = & \frac{\frac{v(t)D(t)\sin\gamma(t)}{\sin\theta_i\cos\beta(t)}F(t)}{\sin^2\theta_i\cos^2\beta(t) + F^2(t)} \\ & \pm \frac{\sqrt{(1-v^2(t))\left[\sin^2\theta_i\cos^2\beta(t) + F^2(t)\right] - v^2(t)\sin^2\gamma(t)}}{\sin^2\theta_i\cos^2\beta(t) + F^2(t)} \end{aligned} \tag{71}$$

Unfortunately, the above suffers from a numerical divide-by-zero problem for some orbit angles. This problem can be remedied in the following way: rewrite the expression as

$$s(t) = s_1(t) \pm s_2(t), \tag{72}$$

where

$$s_1(t) = \frac{\frac{v(t)D(t)\sin\gamma(t)}{\sin\theta_i\cos\beta(t)}F(t)}{\sin^2\theta_i\cos^2\beta(t) + F^2(t)}, \tag{73}$$

and

$$s_2(t) = \frac{\sqrt{(1-v^2(t))\left[\sin^2\theta_i\cos^2\beta(t) + F^2(t)\right] - v^2(t)\sin^2\gamma(t)}}{\sin^2\theta_i\cos^2\beta(t) + F^2(t)}. \tag{74}$$

One can then rewrite (76) as

$$\hat{\mathbf{u}}_i(t) = v(t)\begin{bmatrix} -\sin\gamma(t) \\ 0 \\ \cos\gamma(t) \end{bmatrix} + \begin{bmatrix} [s_1(t)+s_2(t)]\cos\gamma(t)\cos\beta(t)\sin\theta_i \\ -v(t)\frac{D(t)\sin\gamma(t)}{\sin\theta_i\cos\beta(t)} + s_1(t)F(t) + s_2(t)F(t) \\ [s_1(t)+s_2(t)]\sin\gamma(t)\cos\beta(t)\sin\theta_i \end{bmatrix} \tag{75}$$

which can be simplified to

$$\hat{\mathbf{u}}_i(t) = \begin{bmatrix} -v(t)\sin\gamma(t) + \frac{v(t)D(t)F(t)\cos\gamma(t)\sin\gamma(t)}{F^2(t)+[\sin\theta_i\cos\beta(t)]^2} \pm s_2(t)\cos\gamma(t)\cos\beta(t)\sin\theta_i \\ -\frac{v(t)D(t)\sin\theta_i\sin\gamma(t)\cos\beta(t)}{F^2(t)+[\sin\theta_i\cos\beta(t)]^2} \pm s_2(t)F(t) \\ v(t)\cos\gamma(t) + \frac{v(t)D(t)F(t)\sin^2\gamma(t)}{F^2(t)+[\sin\theta_i\cos\beta(t)]^2} \pm s_2(t)\sin\gamma(t)\cos\beta(t)\sin\theta_i \end{bmatrix} \tag{76}$$

Written this way, the expression for the look vector avoids the computational problem of (61) that arises when $\cos\beta(t) = 0$.

B.3. Representation of the PCR satellite orbit tangent vector in the PCI frame

In order to properly align the azimuth dimension of the radar antenna along the satellite track in the PCR reference frame, it is necessary to compute the orbit tangent vector in the PCR frame. The representation of this vector in the PCI frame is then the vector along which the azimuth axis of the radar antenna should be aligned.

According to [AD4],

$$\dot{\mathbf{x}}_p(t) = \dot{\mathbf{M}}(t)\mathbf{x}_i(t) + \mathbf{M}(t)\dot{\mathbf{x}}_i(t). \tag{77}$$

In the PCI reference system, this vector is represented as

$$\begin{aligned} \mathbf{A}'_z(t) &= \mathbf{M}^T(t)\dot{\mathbf{M}}(t)\mathbf{x}_i(t) + \mathbf{M}^T(t)\mathbf{M}(t)\dot{\mathbf{x}}_i(t) \\ &= \omega_p\mathbf{Q}_2\mathbf{x}_i(t) + \dot{\mathbf{x}}_i(t) \\ &= \omega_p R(t)\mathbf{Q}_2\left[-\cos\gamma(t)\mathbf{n}_i(t) + \sin\gamma(t)\mathbf{t}_i(t)\right] + v_s(t)\mathbf{t}_i(t) \\ &= -\omega_p R(t)\cos\gamma(t)\mathbf{Q}_2\mathbf{n}_i(t) + \left[\omega_p R(t)\sin\gamma(t)\mathbf{Q}_2 + v_s(t)\mathbf{I}\right]\mathbf{t}_i(t) \\ &\propto -\cos\gamma(t)\mathbf{Q}_2\mathbf{n}_i(t) + \left[\sin\gamma(t)\mathbf{Q}_2 + D(t)\mathbf{I}\right]\mathbf{t}_i(t) \end{aligned} \tag{78}$$

The representation of the vector

$$\mathbf{A}_z(t) = -\cos\gamma(t)\mathbf{Q}_2\mathbf{n}_i(t) + \left[\sin\gamma(t)\mathbf{Q}_2 + D(t)\mathbf{I}\right]\mathbf{t}_i(t) \tag{79}$$

in the tcn inertial frame may be calculated by succesively premultiplying by $\mathbf{t}_i(t)$, $\mathbf{n}_i(t)$ and $\mathbf{c}_i(t)$ and using the expressions in (33) to (38) to find that

$$\mathbf{A}_z(t) = \left[D(t) - \cos\gamma(t)\cos\theta_i\right]\mathbf{t}_i(t) - \cos\beta(t)\sin\theta_i\mathbf{c}_i(t) - \sin\gamma(t)\cos\theta_i\mathbf{n}_i(t). \tag{80}$$

This vector has a norm given by

$$|\mathbf{A}_z(t)| = \sqrt{D^2(t) - 2D(t)\cos\gamma(t)\cos\theta_i + \cos^2\theta_i\sin^2\beta(t) + \cos^2\beta(t)} \tag{81}$$

Thus, the representation of the unit PCR tangent vector in the PCI frame, **which is the unit**

vector along which the azimuth axis of the antenna should be aligned, is given by

$$\hat{\mathbf{a}}_i(t) = \frac{1}{|\mathbf{A}_z(t)|}\begin{bmatrix} D(t) - \cos\gamma(t)\cos\theta_i \\ -\cos\beta(t)\sin\theta_i \\ -\sin\gamma(t)\cos\theta_i \end{bmatrix}. \tag{82}$$

This vector is, of course, the unit vector in the direction of $\mathbf{v}_1(t)$ in (55).

C. SIMPLIFICATIONS FOR SPECIAL CASES

This section considers some special cases.

C.1. Circular Orbit

Consider the case of a perfectly circular orbit, $\gamma(t) = 0$, $R(t) = R$, $v_s(t) = v_s = R\omega_o$, where ω_o is the orbit radial velocity. The zero-Doppler constraint becomes

$$\hat{\mathbf{u}}_i^T(t)\begin{bmatrix} \cos\theta_i - \frac{\omega_o}{\omega_p} \\ \sin\theta_i\cos\beta(t) \\ 0 \end{bmatrix} = 0 \tag{83}$$

This can be ensured with an inertial look vector of the form

$$\hat{\mathbf{u}}_i(t) \propto \begin{bmatrix} \sin\theta_i\cos\beta(t) \\ \frac{\omega_o}{\omega_p} - \cos\theta_i \\ C \end{bmatrix} \tag{84}$$

for any constant C.

Note that the yaw angle by which to steer the satellite is a rotation around the $\mathbf{n}_i(t)$ axis. The amount by which to rotate is given by the projection of $\hat{\mathbf{u}}_i(t)$ onto the $\mathbf{c}_i(t) \times \mathbf{t}_i(t)$ plane. The yaw angle is thus given by

$$\tan[Y(t)] = \frac{\hat{\mathbf{u}}_i^T(t)\mathbf{t}_i(t)}{\hat{\mathbf{u}}_i^T(t)\mathbf{c}_i(t)} = \frac{\sin\theta_i\cos\beta(t)}{\frac{\omega_o}{\omega_p} - \cos\theta_i} \tag{85}$$

This is the same result as reported in [RD3–RD7]

C.2. Polar Orbit

In the case $\theta_i = \pi/2$, one arrives at the condition that

$$\hat{\mathbf{u}}_i^T(t) \begin{bmatrix} -\frac{v_s(t)}{\omega_p R(t)} \\ \cos\beta(t) \\ 0 \end{bmatrix} = 0 \tag{86}$$

which can be ensured with an inertial look vector of the form

$$\hat{\mathbf{u}}_i(t) \propto \begin{bmatrix} \cos\beta(t) \\ \frac{v_s(t)}{\omega_p R(t)} \\ C \end{bmatrix} \tag{87}$$

for any constant C. In terms of yaw angle,

$$\tan[Y(t)] = \frac{\hat{\mathbf{u}}_i^T(t)\mathbf{t}_i(t)}{\hat{\mathbf{u}}_i^T(t)\mathbf{c}_i(t)} = \frac{\omega_p R(t)\cos\beta(t)}{v_s(t)} \tag{88}$$

C.3. Circular Polar Orbit

A combination of the previous two special cases is a perfectly circular polar orbit where $\theta_i = \pi/2$, $\gamma(t) = 0$, $R(t) = R$. The zero-Doppler constraint then becomes

$$\hat{\mathbf{u}}_i^T(t) \begin{bmatrix} -\frac{\omega_o}{\omega_p} \\ \cos\beta(t) \\ 0 \end{bmatrix} = 0 \tag{89}$$

which leads to a yaw steering angle of

$$\tan[Y(t)] = \frac{\omega_p}{\omega_o}\cos\beta(t) \tag{90}$$

D. USEFUL ELLIPTICAL ORBIT PROPERTIES

This section seeks to relate the angles (to each other) defined in Figure 9. This material is available in numerous text books, but is here specifically recast into forms useful for zero-Doppler steering.

As illustrated in the figure, the satellite position in the 2-dimensional $\hat{\mathbf{i}}_e, \hat{\mathbf{j}}_e$ reference frame is given

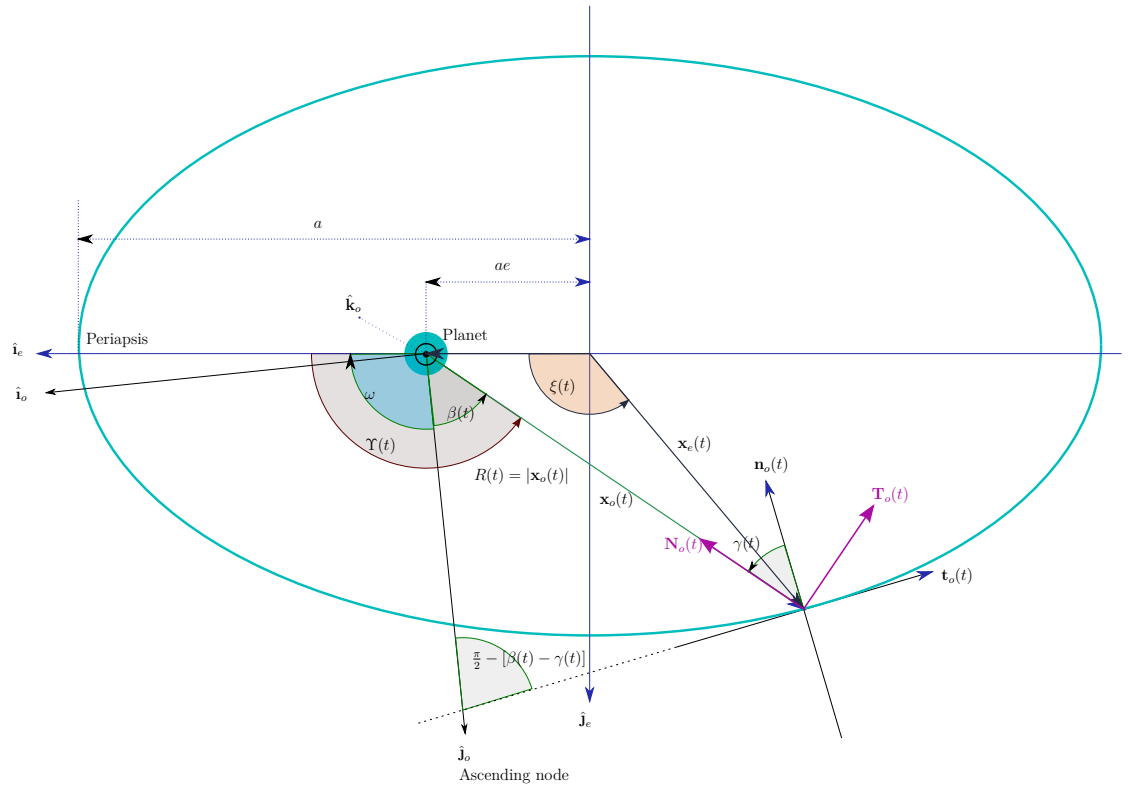

Figure 9: [Satellite-orbit-centered reference frames. Relative to $\hat{\mathbf{j}}_e$, ω denotes the argument of perigee, $\Upsilon(t) = \beta(t) - \omega$ represents the true anomaly, e denotes the orbit eccentricity, a the semi-major axis length, $\mathbf{x}_e(t)$ and $\mathbf{x}_o(t)$ denote the satellite position vector in the OE and VCIP frames, respectively, $\gamma(t)$ represents the angle between tcn and TCN frames.

by

$$\mathbf{x}_e(t) = \begin{bmatrix} a\cos\xi(t) \\ b\sin\xi(t) \end{bmatrix}, \tag{91}$$

where a, b are the semi-major and semi-minor ellipse lengths, respectively, while the center of the planet is located at

$$\mathbf{p} = \begin{bmatrix} ae \\ 0 \end{bmatrix}. \tag{92}$$

With the eccentricity defined as $b^2 = a^2(1 - e^2)$, one calculates that

$$|\mathbf{x}_e(t) - \mathbf{p}| = a[1 - e\cos\xi(t)]. \tag{93}$$

The tangent vector at the satellite position (or the velocity vector) is given by

$$\dot{\mathbf{x}}_e(t) = -\xi'(t) \begin{bmatrix} a\sin\xi(t) \\ -b\cos\xi(t) \end{bmatrix}. \tag{94}$$

This vector has a norm given by

$$|\dot{\mathbf{x}}_e(t)| = a|\xi'(t)|\sqrt{1 - e^2\cos^2\xi(t)}. \tag{95}$$

Because (see Figure 9)

$$\cos[\pi/2 - \gamma(t)] = \frac{[\mathbf{x}_e(t) - \mathbf{p}]^T\dot{\mathbf{x}}_e(t)}{|\mathbf{x}_e(t) - \mathbf{p}||\dot{\mathbf{x}}_e(t)|}, \tag{96}$$

one finds that

$$\sin\gamma(t) = \frac{e\sin\xi(t)}{\sqrt{1 - e^2\cos\xi^2(t)}}, \tag{97}$$

$$\cos\gamma(t) = \frac{\sqrt{1 - e^2}}{\sqrt{1 - e^2\cos\xi^2(t)}}. \tag{98}$$

Note also, from the definition of the satellite point in the ellipse reference frame, with $\Upsilon(t) = \beta(t) - \omega$, where ω is the argument of perigee, that

$$\cos[\beta(t) - \omega] = \cos\Upsilon(t) = \frac{\cos\xi(t) - e}{1 - e\cos\xi(t)}. \tag{99}$$

This can be inverted to show that

$$\cos\xi(t) = \frac{\cos\Upsilon(t) + e}{1 + e\cos\Upsilon(t)} \tag{100}$$

$$\sin\xi(t) = \frac{\sqrt{1 - e^2}\sin\Upsilon(t)}{1 + e\cos\Upsilon(t)}, \tag{101}$$

which ultimately leads to the relations that

$$\cos\gamma(t) = \frac{1 + e\cos[\beta(t) - \omega]}{\sqrt{1 + 2e\cos[\beta(t) - \omega] + e^2}} \tag{102}$$

$$\sin\gamma(t) = \frac{e\sin[\beta(t) - \omega]}{\sqrt{1 + 2e\cos[\beta(t) - \omega] + e^2}} \tag{103}$$

Interesting fact: the expression for $\cos\gamma(t)$ is the same expression as used for pitch control law in [RD6, RD7].

From (93), one also finds that, since $R(t) = |\mathbf{x}_e(t) - \mathbf{p}| = a[1 - e\cos\xi(t)]$,

$$R(t) = \frac{a(1 - e^2)}{1 + e\cos[\beta(t) - \omega]} \tag{104}$$

This expression can be used in the OCS reference frame to determine that

$$\mathbf{x}_o(t) = \frac{a(1-e^2)}{1+e\cos[\beta(t)-\omega]}\begin{bmatrix}-\sin\beta(t)\\ \cos\beta(t)\\ 0\end{bmatrix} \tag{105}$$

The vis-viva equation, [RD8], relates satellite speed to range via

$$v_s^2(t) = GM\left(\frac{2}{R(t)} - \frac{1}{a}\right), \tag{106}$$

where G is the gravitational constant and M is the mass of the planet. After some maniuplation, and by substituting (104) into the above, one finds that

$$v_s(t) = \sqrt{\frac{GM}{a}}\sqrt{\frac{1+2e\cos\Upsilon(t)+e^2}{1-e^2}}. \tag{107}$$

This allows us to express (53) as

$$D(t) = \frac{1}{\omega_p}\sqrt{\frac{GM}{[a(1-e^2)]^3}}\left[1+e\cos\Upsilon(t)\right]\sqrt{1+2e\cos\Upsilon(t)+e^2}. \tag{108}$$

Further, by using equations (94), (100) and (101)

$$\hat{\dot{\mathbf{x}}}_e(t) = \frac{1}{\sqrt{1+2e\cos\Upsilon(t)+e^2}}\begin{bmatrix}-\sin\Upsilon(t)\\ e+\cos\Upsilon(t)\end{bmatrix}, \tag{109}$$

thus

$$\dot{\mathbf{x}}_e(t) = \sqrt{\frac{GM}{a(1-e^2)}}\begin{bmatrix}-\sin\Upsilon(t)\\ e+\cos\Upsilon(t)\end{bmatrix} \tag{110}$$

and

$$\begin{aligned}\dot{\mathbf{x}}_o(t) &= \sqrt{\frac{GM}{a(1-e^2)}}\begin{bmatrix}-\sin\omega & -\cos\omega & 0\\ \cos\omega & -\sin\omega & 0\\ 0 & 0 & 1\end{bmatrix}\begin{bmatrix}-\sin\Upsilon(t)\\ e+\cos\Upsilon(t)\\ 0\end{bmatrix}\\ &= -\sqrt{\frac{GM}{a(1-e^2)}}\begin{bmatrix}\cos\beta(t)+e\cos\omega\\ \sin\beta(t)+e\sin\omega\\ 0\end{bmatrix}\end{aligned} \tag{111}$$

The following relations prove useful in calculations

$$D(t)\cos\gamma(t) = \frac{1}{\omega_p}\sqrt{\frac{GM}{[a(1-e^2)]^3}}\left(1+e\cos[\beta(t)-\omega]\right)^2 \tag{112}$$

$$D(t)\sin\gamma(t) = \frac{e}{\omega_p}\sqrt{\frac{GM}{[a(1-e^2)]^3}}\left(1+e\cos[\beta(t)-\omega]\right)\sin[\beta(t)-\omega] \tag{113}$$

D.1. Orbit angle and time

This section aims to transform the orbit angle in the orbit plane into a time offset so that a relation between the inertial and rotating reference frame can be computed.

We start by equating the satellite velocity from (95) to the result from the vis-viva equation, (107), to find that

$$a|\xi'(t)|\sqrt{1-e^2\cos^2\xi(t)} = \sqrt{\frac{GM}{a}}\sqrt{\frac{1+2e\cos\Upsilon(t)+e^2}{1-e^2}} \tag{114}$$

which, after making a substitution for $\cos\xi(t)$ by applying (100), yields

$$|\xi'(t)| = \sqrt{\frac{GM}{a}}\frac{1}{a(1-e^2)}\left[1+e\cos\Upsilon(t)\right]. \tag{115}$$

One also finds, by taking the derivative of (100) with respect to t, that

$$\xi'(t)\sin\xi(t) = \frac{\Upsilon'(t)\sin\Upsilon(t)(1-e^2)}{\left[1+e\cos\Upsilon(t)\right]^2}. \tag{116}$$

This can be simplified to give

$$\xi'(t) = \frac{\Upsilon'(t)\sqrt{1-e^2}}{1+e\cos\Upsilon(t)}, \tag{117}$$

which can be equated with (115) to yield the following differential equation

$$\mathrm{d}\Upsilon(t) = \pm\sqrt{\frac{GM}{[a(1-e^2)]^3}}\left[1+e\cos\Upsilon(t)\right]^2\mathrm{d}t. \tag{118}$$

This equation may be written as

$$\frac{\mathrm{d}\Upsilon(t)}{\left[1+e\cos\Upsilon(t)\right]^2} = \pm\sqrt{\frac{GM}{[a(1-e^2)]^3}}\mathrm{d}t, \tag{119}$$

and both sides can be integrated. Note that we can choose the positive sign in the above because the inclination angle defines whether the orbit is pro or retrograde. The solution, according to

formulas 2.554.3 and 2.553.3 in [RD9], is given by

$$\frac{2}{\sqrt{1-e^2}}\tan^{-1}\left(\frac{(1-e)\tan\frac{\Upsilon(t)}{2}}{\sqrt{1-e^2}}\right)-\frac{e\sin\Upsilon(t)}{1+e\cos\Upsilon(t)}=t\sqrt{\frac{GM}{a^3(1-e^2)}} \tag{120}$$

This expression allows for calculation of t given the angle $\Upsilon(t)$. Finding $\Upsilon(t)$ given t can be done numerically; indeed, the derivative of t with respect to Υ is given by (118). Thus in iterative approach may be given by

$$\Upsilon_{n+1}=\Upsilon_n+[t-t(\Upsilon_n)]\sqrt{\frac{GM}{[a(1-e^2)]^3}}\,[1+e\cos\Upsilon_n]^2 \tag{121}$$

or, to next order

$$\Upsilon_{n+1}=\Upsilon_n-\frac{1+e\cos\Upsilon_n}{2e\sin\Upsilon_n}\left[1\pm\sqrt{1+4e\sqrt{\frac{GM}{[a(1-e^2)]^3}}\sin\Upsilon_n(1+e\cos\Upsilon_n)\,[t-t(\Upsilon_n)]}\right] \tag{122}$$